Journal of the Meteorological Society of Japan

EARLY ONLINE RELEASE

The DOI for this manuscript is
DOI:10.2151/jmsj.2024-016
J-STAGE Advance published date: February 27th, 2024
The final manuscript after publication will replace the preliminary version at the above DOI once it is available.

Physical Properties of Background Aerosols and Cloud Condensation Nuclei Measured in Kochi City in June 2010 and Its Implication for Planned and Inadvertent Cloud Modification

Katsuya YAMASHITA[*1]**, Wei-Chen KUO**
Meteorological Research Institute, Tsukuba, Japan

Masataka MURAKAMI
Institute for Space-Earth Environmental Research, Nagoya University, Nagoya, Japan
Typhoon Science and Technology Research Center, Yokohama National University, Yokohama, Japan
Meteorological Research Institute, Tsukuba, Japan

Takuya TAJIRI, Atsushi SAITO[*2]**, Narihiro ORIKASA, and Hideaki OHTAKE**[*3]
Meteorological Research Institute, Tsukuba, Japan

Corresponding author: Masataka Murakami, Institute for Space-Earth Environmental Research, Nagoya University, Furo-cho, Chikusa-ku, Nagoya, Aichi 464-8601, Japan.
Email: mamuraka@mri-jma.go.jp
*1 Current affiliation: Snow and Ice Research Center, National Research Institute for Earth Science and Disaster Resilience, Nagaoka, Japan
*2 Current affiliation: Aerological Observatory, Japan Meteorological Agency, Tsukuba, Japan
*3 Current affiliation: National Institute of Advanced Industrial Science and Technology, Tsukuba, Japan

Abstract

Background (BG) aerosol particles (APs) acting as cloud condensation nuclei (CCN) and/or ice nucleating particles (INPs) influence short-range precipitation forecasts and climate change projections by modulating cloud and precipitation microphysical structures and influence the effects of cloud seeding on precipitation enhancement. However, data on the CCN and INP capabilities of BG APs are limited in terms of geographical locations and time. To investigate the characteristics of BG APs, we conducted ground-based measurements of BG AP and CCN in Kochi City, Japan, in June 2010. Comparisons with previously published data on AP and CCN concentrations in East Asia showed that the mean concentrations of APs and CCN at the observation site were considerably affected by air pollution. Our findings also suggest that during the observation period, even air masses from the Pacific Ocean were considerably affected by air pollution in East Asia, including Japan. Moreover, aircraft-measured AP and CCN concentrations in the boundary layer were comparable to those measured concurrently at the surface observation site, although the horizontal positions of the ground- and aircraft-based measurements were not identical; the size distributions of the APs were similar. These results suggest that ground-based

measurements represent APs and CCN in the boundary layer, where the air is ingested by clouds. Numerical simulations with a detailed bin microphysics parcel model showed that cloud droplet number concentrations, based on meteorological conditions and aerosol characteristics expected near the observation site environments, would range from 500 to 1,500 droplets cm^{-3}. These concentrations were consistent with aircraft measurements. These values are higher than the threshold concentration of ~500 droplets cm^{-3} in clouds suitable for hygroscopic seeding, as suggested by previous studies. Therefore, this area is considered to be suitable for rain enhancement by hygroscopic seeding.

Keywords: cloud condensation nuclei; characteristics of atmospheric aerosols; hygroscopic seeding; weather modification

1. Introduction

The direct and indirect effects of aerosols can modulate vertical profiles and amplitudes of diabatic heating and change global and regional atmospheric circulation. In the climate models, the influence of aerosols on atmospheric circulation has long been investigated primarily from the viewpoint of the direct effect of aerosols. In recent years, it has been recognized that aerosol particles (APs) also act as cloud condensation nuclei (CCN) and/or ice nucleating particles (INPs) that modulate the number density and size of cloud droplets and ice crystals, and thus influence short-range precipitation forecasts and climate change projections. These are brought about by the first (modulating the radiation property of clouds; Twomey 1974) and second (modulating precipitation efficiency, spatial distribution, and lifetime of clouds; Albrecht 1989) aerosol indirect effects. These effects are also being investigated in climate models.

Background (BG) APs that act as CCN and INPs not only affect short-term precipitation forecasts and climate change projections by modulating the microphysical structure of clouds and precipitation but can also compete with seeding aerosols and influence precipitation enhancement by cloud seeding. Therefore, to assess the feasibility of rain enhancement by hygroscopic seeding, understanding the characteristics of BG APs acting as CCN is important. Previous studies have suggested that the effect of hygroscopic seeding depends substantially on the cloud type and atmospheric environment for cloud formation (Reisin et al. 1996; Cooper et al. 1997; Yin et al. 2000; Segal et al. 2004; Kuba and Murakami 2010). Cotton (2009) pointed out that the effect of hygroscopic seeding depends on the hygroscopicity, size, and concentration of BG APs and the seeding material. He also suggested a rough estimate of ~500 droplets cm^{-3} as the threshold value of cloud droplet number concentrations for hygroscopic seeding, based on the results of numerical simulations. However, the data on physicochemical properties, particularly CCN and INP capabilities of BG APs, are still insufficient and their availability is considerably limited in geographical locations and time.

To understand the physicochemical properties of BG APs, partucularly those acting as CCN, and to assess their influence on natural cloud formation and precipitation development and possible effects of hygroscopic seeding, we performed ground-based measurements of BG APs. This was conducted during June 2010 in Kochi City, because it is windward of the target area for precipitation enhancement (Sameura Dam in Shikoku),.

Herein, we present the results of these ground-based measurements. We also discuss the spatial representativeness of ground-based measurements at the Kochi City observation site and the differences in the BG APs and CCN between various air masses in June 2010. The feasibility of hygroscopic seeding over the Kochi area in early summer is also briefly discussed based on the number concentrations of cloud droplets simulated using a detailed bin microphysics parcel model.

2. Observation site and facilities

Harigi (33.54°N, 133.47°E) in Kochi City was selected as the site for ground-based in situ measurements (Fig. 1) because it is the windward area of the catchment area for rain enhancement experiments. The measurement instruments were installed in a prefabricated cabin on the site. As part of the Japanese Cloud Seeding Experiments for Precipitation Augmentation (JCSEPA) project (Murakami et al. 2015), we performed intensive field observations of the physical properties of aerosols and clouds from an instrumented aircraft and by ground-based remote sensing from June 4 to 24, 2010. The instruments used for the ground-based *in-situ* measurements were a scanning mobility particle sizer

(SMPS; Model 3936, TSI Ltd.), which measures the size distribution of APs between 0.01 and 0.3 μm diameter; an optical particle counter (OPC; Model KC-01E, RION Ltd.), which measures the size distribution of APs between 0.3 and 5 μm diameter; and a University of Wyoming CCN counter (CCNC; Snider et al. 2003), which measures the CCN concentrations at multiple supersaturations with respect to water (hereafter, SSw). The time resolutions of the SMPS, OPC, and CCNC were two, one, and two minutes, respectively. The time resolution of the CCNC refers to the supersaturation scan duration at 0.2%, 0.7%, and 1.0% SSw. Air from outside the cabin was introduced into the instruments from an inlet set approximately 3 m above the ground through stainless steel and conductive tubing (total length: 4 m).

As the temperature inside the instruments was usually several degrees higher than the air temperature outside, the relative humidity of the sample air was mostly <50%, and it can be considered that a size close to the dry particle size was measured. The penetration efficiency of particles in an inclined tube under laminar flow conditions was calculated considering gravitational settling, diffusion losses, and loss in a bent section of circular tubing (Willeke and Baron 1993). The particle loss in the sampling tubes was estimated to be negligibly small for submicron particles: 2% for particles of 1 μm and 40% for particles with a diameter of 5 μm. The number concentration of particles that are larger than several micrometers is possibly underestimated, but the penetration coefficient is not corrected in this study. The wind direction, wind speed, and air temperature were observed simultaneously using an automatic weather station (AWS; Climatec Ltd.).

The in-situ measurement aircraft (King Air B200T, Diamond Air Service) was equipped with meteorological instruments (e.g., Rosemount total air temperature sensor, chilled-mirror type dew point hygrometer, and Rosemount gust probe), position and attitude instruments (e.g., GPS receiver and Applanix position and orientation system), cloud physics instruments (e.g., forward scattering spectrometer probe (FSSP); passive cavity aerosol spectrometer probe; cloud, aerosol, and precipitation spectrometer; precipitation imaging probe; cloud particle imager; CSIRO-King liquid water content probe; Gerber particle volume monitor; and Nevzorov total water content/liquid water content probes), and aerosol instruments (e.g., OPC, SMPS, CCNC and an impactor for aerosol sampling on electron microscopic meshes). All instruments used for the aircraft-based measurements of APs were the same as those used for the ground-based measurements, except for the CCNC (Model CCN-200, DMT Ltd.). An isokinetic inlet installed on the top of the aircraft fuselage was used to sample APs. After introducing sample air into the cabin, APs were distributed to each instrument through a manifold. The transmittance of aerosol sampling by the aircraft also yielded values similar to that of the ground-based measurements.

3. Results

3.1 Weather conditions during the observation period

The data collected by the AWS at the observation site showed that the dominant daytime wind direction was southerly to southwesterly and the nighttime direction was southwesterly to westerly. Air masses mainly came directly from the Pacific Ocean or partly through Kyushu, where local pollution is generally low (Kaneyasu et al. 2011). The mean wind speed during the observation period was 1.9 m s^{-1}; however, the standard deviations of wind speed were smaller during the day than at night. The diurnal cycle of air temperature reached a minimum at dawn and a maximum at approximately noon. The maximum mean air temperature (± standard deviation, hereafter SD) of 25.5 °C (±3.1 °C) was reached between 12:00 and 13:00 JST (Supplement 1).

According to the observations at the Kochi Local Meteorological Observatory (33.57°N, 133.55°E), located approximately 6 km east of the observation site, the mean air temperature, cloud amount, relative humidity, and precipitation in June 2010 were 23.3 °C (the climate normal is 22.9 °C), 8.3 (8.1), 80% (77%), and 502.0 mm (346.4 mm), respectively. Therefore, the values recorded in 2010 were slightly higher than the climate normals for June. The Japan Meteorological Agency reported that in 2010, the Baiu season, the rainy season in East Asia caused by a stationary front, in the Shikoku district occurred from June 13 to July 17. During a previous drought year (2005), the mean temperature, cloud amount, relative humidity, and precipitation were 24.3 °C, 7.7, 75%, and 74.0 mm, respectively. Except for precipitation, these values are similar to those reported in 2010. This result indicates that the weather conditions over Kochi City in this drought year were not significantly different from those in a normal year, apart from precipitation.

3.2 Number concentrations of BG APs and CCN

Figure 2a shows the time series of the number concentrations of BG APs and CCN at 0.2% SSw during the observation period. CCN concentrations were measured only during the day (09:00–18:00 JST) because water must be manually supplied to the blotting papers every few hours to keep them moist. Therefore, the CCNC cannot be operated without attendants. During the observation period, the mean number concentrations (±SD) of BG APs from 0.01 to 0.3 μm in diameter and >0.3 μm in diameter and of CCN at 0.2% SSw were 4404 cm^{-3} (±2664 cm^{-3}), 78 cm^{-3} (±50 cm^{-3}), and 602 cm^{-3} (±344 cm^{-3}), respectively. According to Pierce and Adams (2009), typical condensation nuclei (CN) concentrations of continental and maritime air masses are greater than 2000 cm^{-3} and less than 850 cm^{-3}, respectively. The CN concentrations in Kochi City during the observation period suggest a continental-type air mass, even though the dominant southerly to westerly wind direction indicates that the air masses mainly originated from the Pacific Ocean and partly through Kyushu.

The mean number concentrations of BG APs between 0.01 and 0.3 μm in diameter were higher during the daytime than at night, whereas the number concentrations of AP >0.3 μm in diameter were almost constant (Fig. 2b). The mean number concentrations of CCN at 0.2% SSw were higher than that of APs >0.3 μm in diameter, but their diurnal variation was similar to that of APs >0.3 μm.

3.3 Aerosol particle size distributions

The time series of the mode diameters of BG APs during the observation period shows that most of the mode diameters were between 0.05 μm and 0.1 μm. However, certain mode diameters were smaller, suggesting the formation of new secondary particles via gas-to-particle conversion (Supplement 2).

The mean and median size distributions of APs, measured with the SMPS, peaked at a diameter of approximately 0.09 μm during both daytime (06:00–18:00 JST) and nighttime (18:00–06:00 JST), and the mean size distribution showed a second, daytime peak at approximately 0.04 μm. The size distribution of APs with a diameter exceeding 0.3 μm (measured by the OPC) showed a shoulder point at approximately 3.6 μm both daytime and nighttime (Fig. 3). These results show that the size distributions of the BG APs in Kochi City during the observation period were mainly bimodal and occasionally trimodal.

3.4 Activation spectra and hygroscopicity of CCN

The daytime CCN activation spectra during the observation period (Fig. 4a) showed mean (±SD) concentrations at 0.2%, 0.7%, and 1.0% SSw of 602 cm^{-3}

(±344 cm^{-3}), 1733 cm^{-3} (±800 cm^{-3}), and 2319 cm^{-3} (±937 cm^{-3}), respectively. When we fitted the formula $N_{CCN} = C\ (SSw)^k$ (often used to represent a CCN activation spectrum) to the mean data, we obtained a value for C corresponding to the number concentration at 1% SSw of 2324 cm^{-3} and a value for k representing the slope of the activation spectrum of 0.8. These values are typical of continental air masses (Pruppacher and Klett 1997).

We plotted the critical supersaturation against the dry diameter and compared the BG AP data for Kochi City with the data of artificially generated test particles (Fig. 4b). Individual data points and averaged values over 14 days were derived using CCN closure analysis (Sullivan et al. 2009). The data points for BG APs were distributed between the hygroscopicity isolines of 0.01 and 1, and the mean hygroscopicity of BG APs was distributed around the isoline of 0.1. Based on their review of the literature, Andreae and Rosenfeld (2008) reported that the mean AP hygroscopicity values of continental and maritime air masses are 0.3 ± 0.1 and 0.7 ± 0.2, respectively. According to this classification, the hygroscopicity of APs in Kochi City is closer to that of continental air masses than maritime air masses.

3.5 Origin of air masses observed over Kochi city

We performed a backward trajectory analysis to deduce the origins of the air masses because they can affect the CCN spectra around Japan, depending on pressure patterns in East Asia. The backward trajectory analysis was performed using the HYSPLIT model to investigate the origins of the air masses at the observation site during the observation period (Draxler and Rolph 2013). We calculated the 3-day backward trajectory of an air mass at 500 m above mean sea level, as a representative air mass in the atmospheric boundary layer, over the ground observation site at 9:00 and 15:00 Japan time for 14 days during which CCN concentration was measured (Fig. 5a). For this analysis, we divided the area around Japan into continental, coastal, and Pacific regions. On 3 of the 14 days (June 12, 13, and 14), when air masses originated in the Pacific region, the CCN concentrations were lower than those on the days when air masses originated from other regions (Fig. 5b). The median aerosol size distributions in air masses transported from the coastal and Pacific regions were compared (Fig. 5c). The concentrations of APs in the submicron size range were lower in the Pacific than in coastal air masses. Moreover, the median hygroscopicity of APs in the coastal and Pacific air masses was 0.11 and 0.20, respectively.

Finally, we compared the CCN spectra in air masses transported from the coastal and Pacific regions (this study) with those measured at various other East Asian and Pacific sites (Fig. 6). The results showed that CCN concentrations decreased with increasing distance from the continent, even though the measurements were obtained during different seasons and years. The CCN concentrations in air masses transported from the coastal and Pacific regions (measured in this study) were comparable with those measured in Tokyo and Cape Hedo, Japan. Takami et al. (2007) suggested that CCN concentrations at Cape Hedo are strongly influenced by the Asian outflow of polluted air, and Kondo et al. (2010) suggested that CCN concentrations in Tokyo reflect local air pollution because Tokyo is a megacity where large amounts of APs and their precursor gases are emitted. Because the CCN values measured at both Cape Hedo and Tokyo were heavily influenced by anthropogenic aerosols, the CCN measured in Kochi City may also reflect the influence of air pollution, even though the dominant wind direction during the study period was from the Pacific Ocean.

4. Discussion

4.1 Spatial representativeness of the BG APs from the ground-based

measurements

Because the indirect effects of aerosols on clouds and precipitation (and hygroscopic seeding effectiveness) depend on the hygroscopicity, size, and number concentration of BG APs (and seeding particles), understanding the characteristics of BG APs in the convective boundary layer that are ingested into clouds is important. Therefore, we examined the spatial representativeness of BG APs obtained from ground-based measurements of APs in the convective boundary layer by comparing them with data collected by simultaneous *in-situ* aircraft measurements.

Eight aircraft flights that collected the data used for comparison with ground-based measurements were synchronous with the ground-based measurements. Although the aircraft flew over ocean and land (Supplement 3), there was little difference in AP and CCN concentrations between the ocean and land.

The distributions of AP and CCN concentrations at 0.7% SSw, averaged over 500-m height intervals, were comparable with ground-based measurements (Fig. 7), although the exact horizontal positions of the ground- and aircraft-based measurements were different. The AP size distributions obtained from the ground- and aircraft-based measurements were also similar (not shown), suggesting that the APs were well mixed within the boundary layer (below 2 km).

From these results, we conclude that BG AP and CCN concentrations obtained from ground-based measurements in this study are representative of the BG APs and CCN in the boundary layer over the Kochi area during the daytime in June 2010. Therefore, they can be used to simulate by numerical models the planned and inadvertent modification of clouds and precipitation due to aerosols.

4.2 Effect of BG APs on clouds

To investigate the effects of BG APs on cloud microphysics, the deliquescence and activation of APs and subsequent condensation and collision–coalescence growth of droplets during adiabatic ascents are simulated using a detailed bin microphysics parcel model. To simulate such processes, the parcel model of Chen and Lamb (1994) was modified to include the κ-Köhler theory of Petters and Kreidenweis (2007) instead of the classical Köhler theory (Yamashita et al. 2011).

The size distribution fitting of the data into a lognormal distribution, as shown in Fig. 8, was used as the initial BG AP size distribution for the model simulation. The median (MID), 10th (LOW), and 90th (HIGH) percentile values were used as the initial BG AP size distributions. The MID and LOW size distributions were approximated using the bimodal size distribution, and the HIGH size distribution was approximated using a trimodal size distribution (Table 1). The hygroscopicity of the background APs was assumed to be 0.1 regardless of particle size.

The initial values of pressure, temperature, and relative humidity for the simulation were 1011.6 hPa, 23.3 °C, and 80%, respectively. These are the mean values observed at the Kochi Local Meteorological Observatory in June 2010. The ascent speeds of the air parcels were assumed to be 0.5, 1, and 2 m s^{-1}, which are within the range of updraft velocities frequently obtained from aircraft observations just below the cloud bases.

Figure 9 shows the vertical distributions of temperature, supersaturation with respect to water, droplet number concentrations, and droplet size distributions at 500 and 600 m obtained from the model simulation when LOW, MID, and HIGH aerosol size distributions with their hygroscopicity of 0.1 were input as the initial BG APs and updraft velocity was set at 1.0 m s^{-1}. The model simulates a cumulus cloud, whose base height is approximately 480 m, and the simulation continues until approximately 500 m above the cloud base, where the effects of entrainment are thought to be small in the updraft core. The simulations with initial HIGH APs approximated by tri-modal and bi-modal size distributions showed no significant difference. This meant that APs in the third mode with a mode diameter of 0.04 μm did not activate cloud droplets.

The maximum cloud droplet number concentration just above the cloud base, which is expected from BG APs and updrafts of 0.5–2 m s^{-1}, is distributed between 400 and 2400 cm^{-3} and centered at 1,200 cm^{-3} (Table 2). Excluding high cloud droplet number concentrations above 1500 cm^{-3} produced under conditions of a combination of the 90th percentile particle size distribution (HIGH AP concentration) and a relatively large updraft of 2 m s^{-1}, the model predictions are consistent with aircraft observations (Fig. 10). This result indicates that most of the clouds ingesting BG APs measured in Kochi City were comprised of cloud droplets with concentrations of 500–1500 cm^{-3}. A cloud droplet concentration of > 500 cm^{-3} indicates the possibility of precipitation enhancement by hygroscopic seeding (Cotton et al. 2009)

5. Conclusions

In June 2010, we conducted ground-based measurements of the BG APs and CCN at an observation site in Kochi City (33.54°N, 133.47°E), windward of a target area for hygroscopic seeding (Sameura Dam).

The mean concentration of APs during the observation period was 4404 cm^{-3} for particles with diameters ranging between 0.01 and 0.3 μm, 78 cm^{-3} for particles > 0.3 μm diameter, and 0.51 cm^{-3} for particles > 1.0 μm diameter. The mean AP size distribution was bimodal with peaks at diameters of 0.09 and 2 μm, or trimodal with peaks at diameters of 0.04, 0.09, and 2 μm. The mean CCN concentrations at 0.2%, 0.7%, and 1.0% SSw were 602 cm^{-3}, 1733 cm^{-3}, and 2319 cm^{-3}, respectively. The mean hygroscopicity derived from the size distributions of the BG APs and CCN activation spectra was approximately 0.1.

A comparison of our data with AP and CCN measurements made at other East Asian sites and reported in the literature suggests that air masses over the Kochi area (below 2 km), including air masses from the Pacific Ocean, during the observation period were highly influenced by anthropogenic aerosols produced in East Asia, including Japan.

Although the exact horizontal positions of the ground- and aircraft-based measurements did not coincide, the observed number concentrations of the BG APs and CCN were comparable. The size distributions of APs were similar between the two datasets. These results suggest that the characteristics of BG

APs obtained from ground-based measurements in Kochi City can be considered representative of AP characteristics in the boundary layer (below 2 km) over the Kochi area and can be closely related to the microphysics of the clouds.

Numerical simulations using a detailed bin spectral microphysics parcel model indicated that most of the clouds ingesting BG APs measured in Kochi City had cloud droplet concentrations of 500–1500 cm^{-3}, which exceeded the criteria for droplet number concentrations suitable for hygroscopic seeding, 500 cm^{-3} (Cotton 2009). Therefore, this area seems suitable for hygroscopic seeding.

The size distribution and hygroscopicity of the BG APs measured in this study may also be useful for future numerical model simulations for warm-cloud seeding using hygroscopic particles over the Kochi area.

Acknowledgments

The authors thank Dr. Michihiko Mochida at Nagoya University for providing us with the CCN spectral data measured at Hedo and in the western Pacific region.

The detailed bin microphysics parcel model used in this study is based on Chen and Lamb's (1994) model, and the cloud physics researchers around Tokyo

(Drs. Naomi Kuba, Ryohei Misumi, Narihiro Orikasa, Akihiro Hashimoto, Takuya Tajiri, Atsushi Saito, Katsuya Yamashita, Masataka Murakami) evaluated the performance of the program provided by Dr. J-P Chen, modified it as necessary, and added certain new functions.

This study was partly supported by the Ministry of Education, Culture, Sports, Science, and Technology of Japan under the program of Special Coordination Funds for Promoting Science and Technology, "Japanese Cloud Seeding Experiments for Precipitation Augmentation (JCSEPA)." This work was also partly supported by JSPS KAKENHI, Grant Numbers 23244095 and 17H0078.

Data Availability Statement

The ground-based aerosol measurement, aircraft observation, and numerical simulation data analyzed in this study are available from the corresponding author on reasonable request.

Supplementary Material

Supplement 1 shows mean diurnal cycles of wind direction, wind speed, and air temperature during the observation period. Supplement 2 shows time series of size distributions and mode diameters of aerosol particles during the observation period. Supplement 3 shows aircraft flight tracks that collected data used for comparison with ground-based measurements.

References

Albrecht, B. A., 1989: Aerosols, cloud microphysics, and fractional cloudiness. *Science*, **245**, 1227–1230.

Andreae M. O., and D. Rosenfeld, 2008: Aerosol–cloud–precipitation interactions. Part 1. The nature and sources of cloud-active aerosols. *Earth Sci. Rev.*, **89**, 13–41.

Chen, J.–P., and D. Lamb, 1994: The theoretical basis for the parameterization of ice crystal habits: Growth by vapor deposition. *J. Atmos. Sci.*, **51**, 1206–1222.

Cooper, W. A., R. T. Bruintjes, and G. K. Mather, 1997: Calculations pertaining to hygroscopic seeding with flares. *J. Appl. Meteor.*, **36**, 1449–1469.

Cotton W. R., 2009: Parallels and contrasts between deliberate cloud seeding and aerosol pollution effects. Aerosol Pollution Impact on Precipitation:

A Scientific Review, Z. Levin and W. R. Cotton, Eds., Springer, 277–294.

Draxler, R. R., and G. D. Rolph, 2013: HYSPLIT (HYbrid Single-Particle Lagrangian Integrated Trajectory) Model access via NOAA ARL READY Website (http://www.arl.noaa.gov/HYSPLIT.php). NOAA Air Resources Laboratory, College Park, MD.

Kaneyasu, N., A. Takami, K. Sato, S. Hatakeyama, M. Hayashi, K. Hara, K. Kawamoto, and S. Yamamoto, 2011: Year-round behavior of PM2.5 in a remote island and urban sites in the northern Kyushu area, Japan, *J. Japan. Soc. Atmos. Environ*., **46**, 111–117.

Kondo, Y., N. Takegawa, H. Matsui, T. Miyakawa, M. Koike, Y. Miyazaki, Y. Kanaya, M. Mochida, M. Kuwata, Y. Morino, and M. Shiraiwa, 2010: Formation and transport of aerosols in Tokyo in relation to their physical and chemical properties: A review. *J. Meteor. Soc. Japan*, **88**, 597-624.

Kuba, N., and M. Murakami, 2010: Effect of hygroscopic seeding on warm rain clouds – numerical study using a hybrid cloud microphysical model. *Atmos. Chem. Phys.*, **10**, 3335-3351.

Kuwata, M., and Y. Kondo, 2008a, Dependence of size-resolved CCN spectra on the mixing state of nonvolatile cores observed in Tokyo. *J. Geophys. Res.*, **113**, D19202, doi:10.1029/2007JD009761.

Kuwata, M., Y. Kondo, Y. Miyazaki, Y. Komazaki, J. H. Kim, S. S. Yum, H. Tanimoto, and H. Matsueda, 2008b: Cloud condensation nuclei activity at Jeju Island, Korea in spring 2005. *Atmos. Chem. Phys.*, **8**, 2933-2948.

Mochida, M., C. Nishita‐Hara, Y. Kitamori, S. G. Aggarwal, K. Kawamura, K. Miura, and A. Takami, 2010: Size‐segregated measurements of cloud condensation nucleus activity and hygroscopic growth for aerosols at Cape Hedo, Japan, in spring 2008. *J. Geophys. Res.*, **115**, D21207, doi:10.1029/2009JD013216.

Mochida, M., C. Nishita‐Hara, H. Furutani, Y. Miyazaki, J. Jung, K. Kawamura, and M. Uematsu, 2011: Hygroscopicity and cloud condensation nucleus activity of marine aerosol particles over the western North Pacific. *J. Geophys. Res.*, **116**, D06204, doi:10.1029/2010JD014759.

Murakami, M., F. Fujibe, and M. Ishihara, 2015: Frontier of Weather Modification Research. Meteorological Research Note, Meteorological Society of Japan, 340pp. (in Japanese).

Petters, M. D., and S. M. Kreidenweis, 2007: A single parameter representation of hygroscopic growth and cloud condensation nucleus activity. *Atmos. Chem. Phys.*, **7**, 1961-1971, doi:10.5194/acp-7-1961-2007.

Pierce, J. R., and P. J. Adams, 2009: Uncertainty in global CCN concentrations from uncertain aerosol nucleation and primary emission rates. *Atmos. Chem. Phys.*, **9**, 1339-1356.

Pruppacher, H. R., and J. D. Klett, 1997: Microphysics of Clouds and Precipitation. Reidel, Dordrecht. 954 pp.

Reisin T., S. Tzivion, and Z. Levin, 1996: Seeding convective clouds with ice nuclei or hygroscopic particles: A numerical study using a model with detailed microphysics. *J. Appl. Meteor.*, **35**, 1416-1434.

Rose, D., A. Nowak, P. Achtert, A. Wiedensohler, M. Hu, M. Shao, Y. Zhang, M. O. Andreae, and U. Pöschl, 2010: Cloud condensation nuclei in polluted air and biomass burning smoke near the mega-city Guangzhou, China – Part 1: Size-resolved measurements and implications for the modeling of aerosol particle hygroscopicity and CCN activity. *Atmos. Chem. Phys.*, **10**, 3365-3383.

Segal, Y., A. Khain, M. Pinsky, and D. Rosenfeld, 2004: Effects of hygroscopic seeding on raindrop formation as seen from simulations using a 2000-bin spectral cloud parcel model. *Atmos. Res.* **72**, 3–35.

Snider, J. R., S. Guibert, J.-L. Brenguier, and J.-P. Putaud, 2003: Aerosol activation in marine stratocumulus clouds: 2. Köhler and parcel theory closure studies. *J. Geophys. Res.*, **108(D15)**, 8629, doi:10.1029/2002JD002692.

Sullivan, R. C., M. J. K. Moore, M. D. Petters, S. M. Kreidenweis, G. C. Roberts, and K. A. Prather, 2009: Effect of chemical mixing state on the hygroscopicity and cloud nucleation properties of calcium mineral dust particles. *Atmos. Chem. Phys.*, **9**, 3303–3316.

Takami, A., T. Miyoshi, A. Shimono, N. Kaneyasu, S. Kato, Y. Kajii, and S. Hatakeyama, 2007: Transport of anthropogenic aerosols from Asia and subsequent chemical transformation. *J. Geophys. Res.*, **112**, D22S31, doi:10.1029/2006JD008120.

Twomey, S., 1974: Pollution and the planetary albedo. *Atmos. Environ*., **8**, 1251–1256.

Willeke, K. and P. A. Baron, 1993: Aerosol measurement: Principles, techniques, and applications. Van Nostrand Reinhold, New York, 876 pp.

Yin, Y., Z. Levin, T. G. Reisin, and S. Tzivion, 2000: Seeding convective clouds with hygroscopic flares; Numerical simulations using a cloud model with detailed microphysics. *J. Apply. Meteor.*, **39**, 1460-1472.

Yamashita K., M. Murakami, A. Hashimoto, and T. Tajiri, 2011: CCN ability of Asian mineral dust particles and their effects on cloud droplet formation. *J. Meteor. Soc. Japan*, **89**, 581-587.

Zhang, Q., J. Meng, J. Quan, Y. Gao, D. Zhao, P. Chen, and H. He, 2012: Impact of aerosol composition on cloud condensation nuclei activity. *Atmos. Chem. Phys.*, **12**, 3783-3790, doi:10.5194/acp-12-3783-2012.

List of Figures

Fig. 4 (a) Activation spectra of CCN during the observation period. Error bars show standard deviations. (b) Relationship between critical water supersaturation and dry diameter. The oblique lines are hygroscopicity isolines. ATD in the legend stands for Arizona Test Dust which is often used as the reference dust particles.

Fig. 5 (a) Three-day backward trajectories from a point 500 m above the observation site at 09:00 JST (red) and 15:00 JST (blue). G, Ti, J, H, To, and K indicate the locations of the Guanzhou, Tianjin, Jeju, Hedo, Tokyo, and Kochi observation sites, respectively. The CCN activation spectra measured at these locations are shown in Fig. 12. (b) Time series of CCN concentrations at 0.2% (○), 0.7% (△), and 1.0% (□) SSw. The symbols and error bars represent the mean and standard deviation, respectively, of one day's data. The vertical gray bar indicates the days on which the air mass was transported from the Pacific region. (c) Median aerosol particle size distributions measured in air masses transported from the coastal and Pacific regions.

Fig. 6 CCN spectra measured in air masses transported from the coastal (▲) and Pacific (▲) regions in this study and those measured at Guangzhou, China (22.55° N, 113.07° E; Rose et al. 2010) in summer 2006, Tianjin, China (39.08° N, 117.20° E; Yin et al. 2012) in autumn 2010, Jeju, Korea (33.20°N, 126.10°E; Kuwata et al. 2008b) in spring 2005, Tokyo, Japan (35.66°N, 139.66°E; Kuwata et al. 2008a) in winter 2007, West Pacific (10-40°N, 155°E; Mochida et al. 2011) in autumn 2008, and Hedo, Japan (26.87N, 128.24E; Mochida et al. 2010) in spring 2008. The error bars represent standard deviations.

Fig. 7 Vertical distributions of concentrations of aerosol particles with diameters ranging from 0.01 to 0.3 μm (left), CCN at 0.7% SSw (middle), and aerosol particles with diameters >0.3 μm (right) averaged over 500-m height intervals. The error bars represent standard deviations. The measurement dates (mm/dd) are shown in the legend. The triangular plots below 500 m altitude indicate the values from the ground observation.

Fig. 8 Median, 90th, and 10th percentile size distributions of background APs (dotted lines) and their log-normal fits (solid lines).

Fig. 9 Vertical distributions of (a) temperature, relative humidity, (b) droplet concentrations, and (c) droplet size distributions at 500 (upper) and 600 (lower) m obtained from the model simulation with median background AP size distribution and updraft velocity of 1 m s^{-1}.

Fig. 10 Frequency of maximum cloud droplet number concentrations measured by the FSSP during the aircraft observation campaign in 2010.

List of Tables

Table 1 Parameters of each log-normal size distribution that constitutes the multi-modal BG AP size distributions for 90th percentile (HIGH), median (MED), and 10 percentile (LOW) values.

Table 2 Dependency of maximum cloud droplet number concentrations and water supersaturation on aerosol number concentration and updraft velocity.

Supplements

SFig. 1 Mean diurnal cycles of wind direction (WD), wind speed (WS), and air temperature during the observation period. Error bars show standard deviations.

SFig. 2 Time series of size distributions (shading) and mode diameters (dots) of aerosol particles during the observation period.

SFig. 3 Aircraft flight tracks that collected data used for comparison with ground-based measurements.

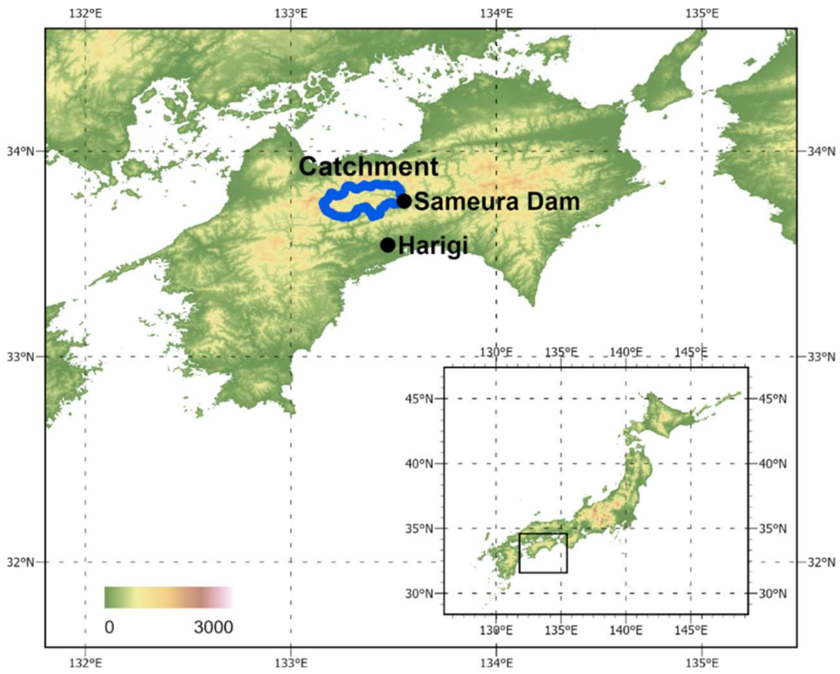

Fig. 1 Map showing the observation site locations in Kochi city and the Sameura Dam catchment area in Shikoku district.

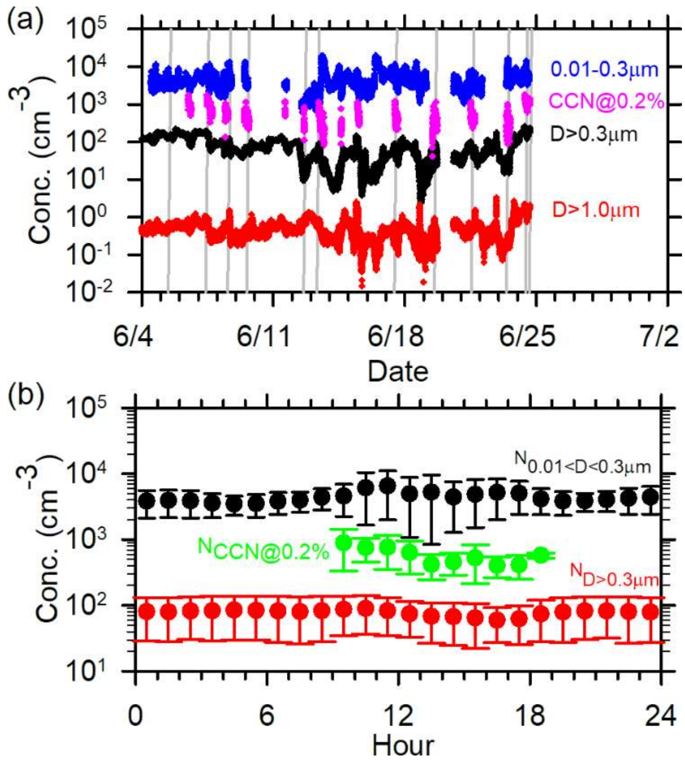

Fig. 2 (a) Time series of the number concentrations of three size classes of aerosol particles (0.01–0.3 μm, >0.3 μm, and >1.0 μm) and CCN at 0.2% SSw during the observation period. The large tick marks in horizontal axis indicate midnight (12:00 AM). The vertical gray bars indicate times when aircraft observations were made. (b) Mean diurnal cycles of the number concentrations of APs with diameters of 0.01–0.3 μm and >0.3 μm and CCN at 0.2% SSw during the observation period. The error bars represent standard deviations.

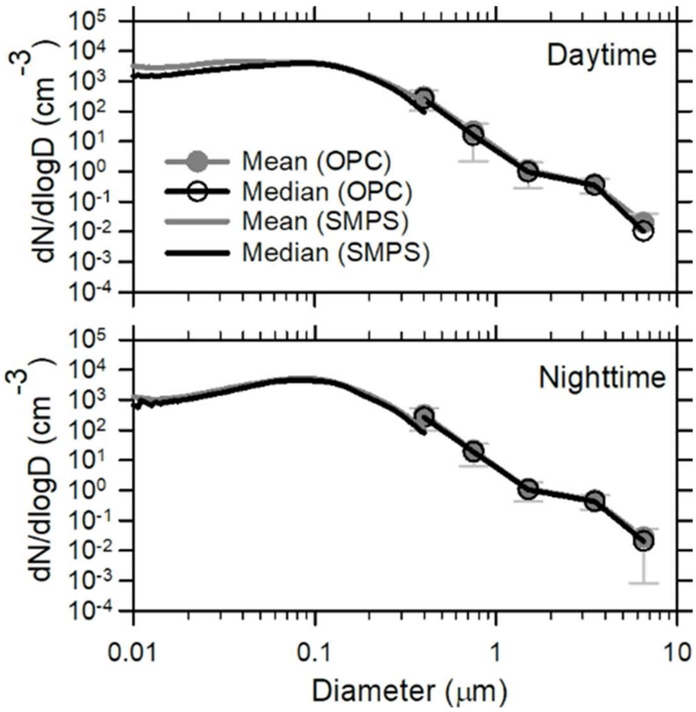

Fig. 3 Daytime (06:00–18:00 JST) and nighttime (18:00–06:00 JST) mean and median size distributions during the observation period measured with the SMPS (diameters from 0.01 to 0.3 μm) and the OPC (0.3 to 5.0 μm).

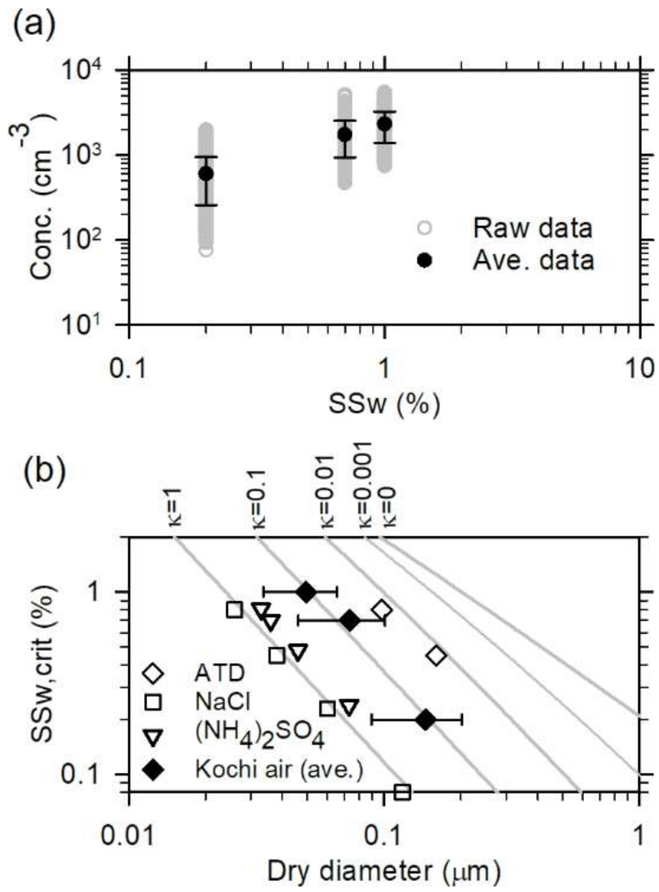

Fig. 4 (a) Activation spectra of CCN during the observation period. Error bars show standard deviations. (b) Relationship between critical water supersaturation and dry diameter. The oblique lines are hygroscopicity isolines. ATD in the legend stands for Arizona Test Dust which is often used as the reference dust particles.

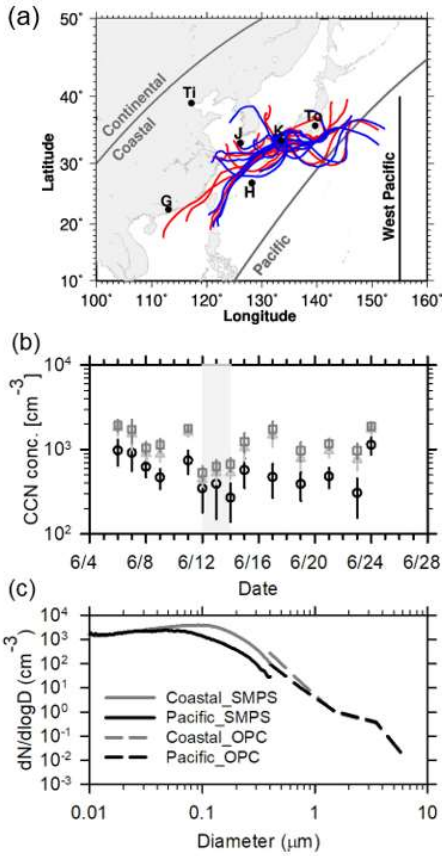

Fig. 5 (a) Three-day backward trajectories from a point 500 m above the observation site at 09:00 JST (red) and 15:00 JST (blue). G, Ti, J, H, To, and K indicate the locations of the Guanzhou, Tianjin, Jeju, Hedo, Tokyo, and Kochi observation sites, respectively. The CCN activation spectra measured at these locations are shown in Fig. 6. (b) Time series of CCN concentrations at 0.2% (○), 0.7% (△), and 1.0% (□) SSw. The symbols and error bars represent the mean and standard deviation, respectively, of one day's data. The vertical gray bar indicates the days on which the air mass was transported from the Pacific region. (c) Median aerosol particle size distributions measured in air masses transported from the coastal and Pacific regions.

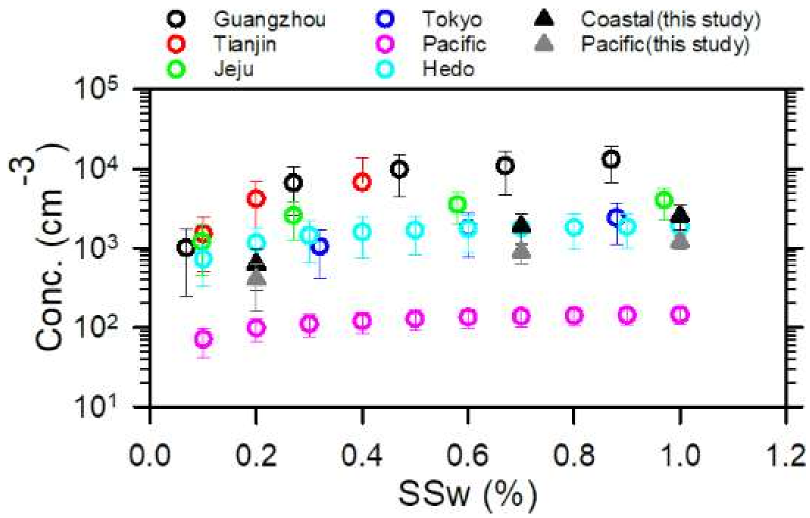

Fig. 6 CCN spectra measured in air masses transported from the coastal (▲) and Pacific (▲) regions in this study and those measured at Guangzhou, China (22.55° N, 113.07° E; Rose et al. 2010) in summer 2006, Tianjin, China (39.08° N, 117.20° E; Yin et al. 2012) in autumn 2010, Jeju, Korea (33.20°N, 126.10°E; Kuwata et al. 2008b) in spring 2005, Tokyo, Japan (35.66°N, 139.66°E; Kuwata et al. 2008a) in winter 2007, West Pacific (10-40°N, 155°E; Mochida et al. 2011) in autumn 2008, and Hedo, Japan (26.87N, 128.24E; Mochida et al. 2010) in spring 2008. The error bars represent standard deviations.

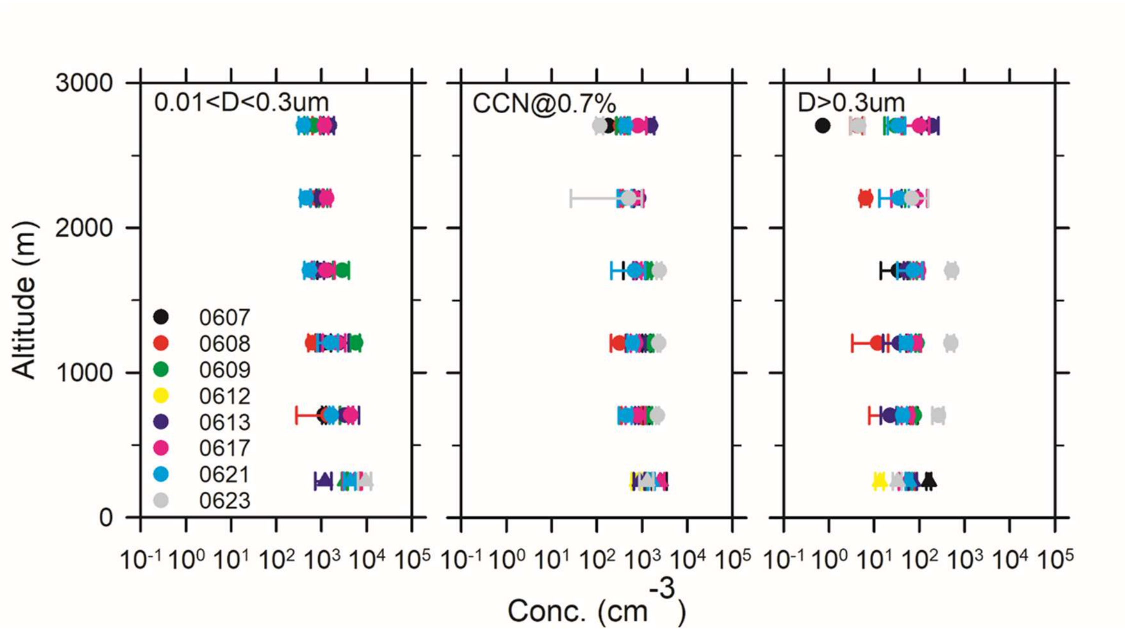

Fig. 7 Vertical distributions of concentrations of aerosol particles with diameters from 0.01 to 0.3 μm (left), CCN at 0.7% SSw (middle), and aerosol particles with diameters >0.3 μm (right) averaged over 500-m height intervals. The error bars represent standard deviations. The measurement dates (mmdd) are shown in the legend. The triangular plots below 500 m altitude indicate the values from the ground observation.

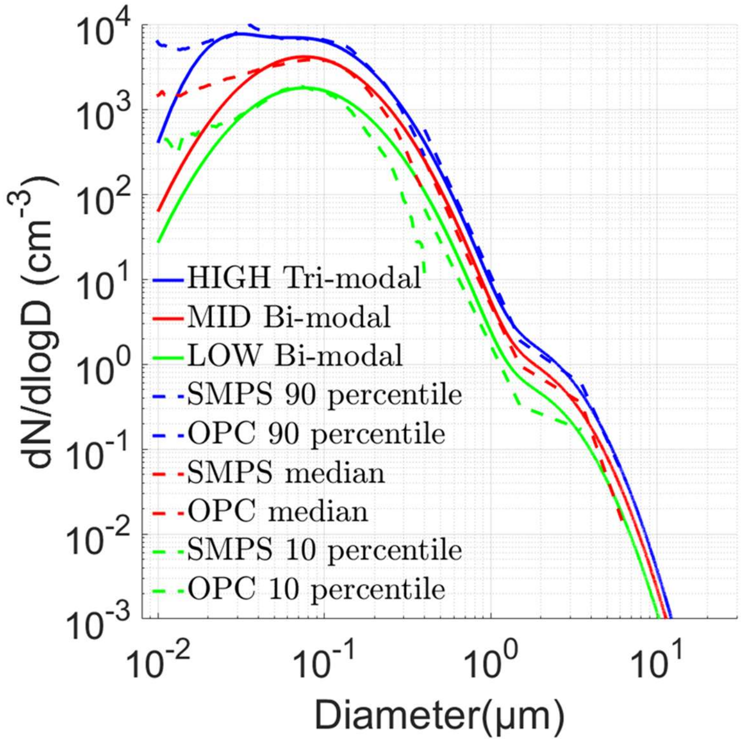

Fig. 8 Median, 90th, and 10th percentile size distributions of background APs (dotted lines) and their log-normal fits (solid lines).

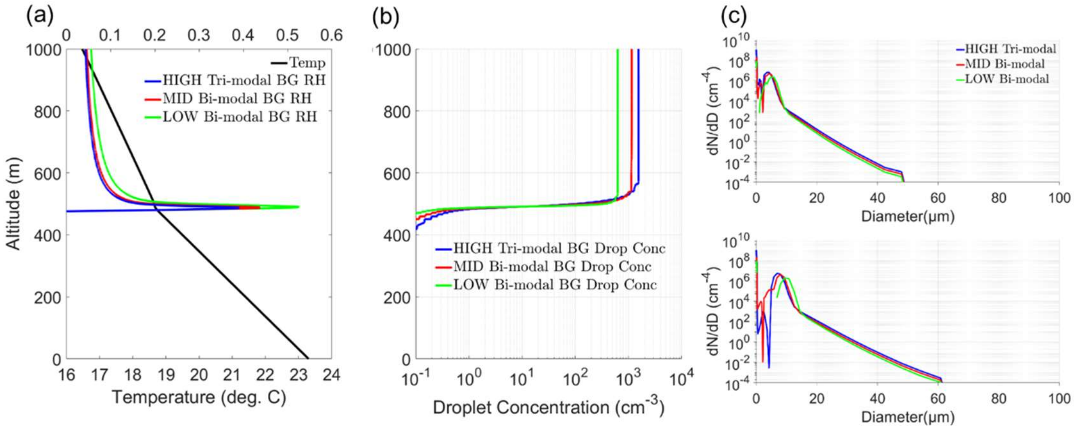

Fig. 9 Vertical distributions of (a) temperature, relative humidity, (b) droplet concentrations, and (c) droplet size distributions at 500 (upper) and 600 (lower) m obtained from the model simulation with median background AP size distribution and updraft velocity of 1 m s^{-1}.

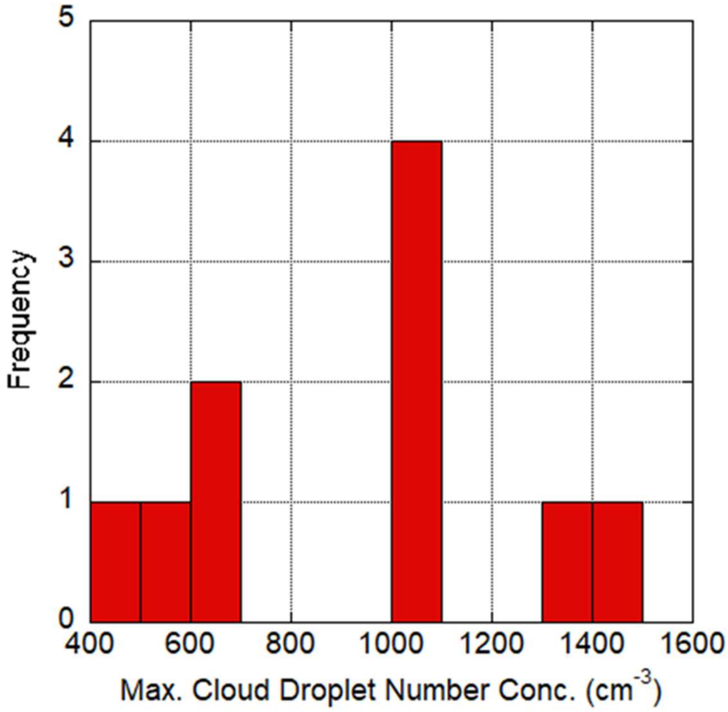

Fig. 10 Frequency of maximum cloud droplet number concentrations measured by the FSSP during the aircraft observation campaign in 2010.

Table 1 Parameters of each log-normal size distribution that constitutes the multi-modal BG AP size distributions for 90th percentile (HIGH), median (MED), and 10th percentile (LOW) values.

	1st mode dia. (m)	1st mode conc. (cm^{-3})	1st mode sigma	2nd mode dia. (m)	2nd mode conc. (cm^{-3})	2nd mode sigma	3rd mode dia. (m)	3rd mode conc. (cm^{-3})	3rd mode sigma
HIGH	1.48e-6	0.92	0.55	7.6e-7	5148	0.7	0.26e-7	2264	0.40
MED	1.48e-6	0.52	0.55	7.6e-7	3158	0.7			
LOW	1.48e-6	0.29	0.55	7.6e-7	1358	0.7			

Table 2 Dependency of maximum cloud droplet number concentrations and water supersaturation on aerosol number concentration and updraft velocity.

Droplet Conc. (cm^{-3}) (SSw (%))	Updraft 0.5 ms^{-1}	Updraft 1.0 ms^{-1}	Updraft 2.0 ms^{-1}
HIGH tri-modal	1037 (0.283)	1545 (0.391)	2444 (0.543)
CNTL bi-modal	784 (0.319)	1151 (0.438)	1609 (0.607)
LOW bi-modal	463 (0.384)	627 (0.526)	800 (0.730)

Supplement for “Physical Properties of Background Aerosols and Cloud Condensation Nuclei Measured in Kochi City in June 2010 and Its Implication for Planned and Inadvertent Cloud Modification”

Katsuya YAMASHITA[*1], Wei-Chen KUO
Meteorological Research Institute, Tsukuba, Japan

Masataka MURAKAMI
Institute for Space-Earth Environmental Research, Nagoya University, Nagoya, Japan
Typhoon Science and Technology Research Center, Yokohama National University, Yokohama, Japan
Meteorological Research Institute, Tsukuba, Japan

Takuya TAJIRI, Atsushi SAITO[*2], Narihiro ORIKASA, and Hideaki OHTAKE[*3]
Meteorological Research Institute, Tsukuba, Japan

Supplement 1

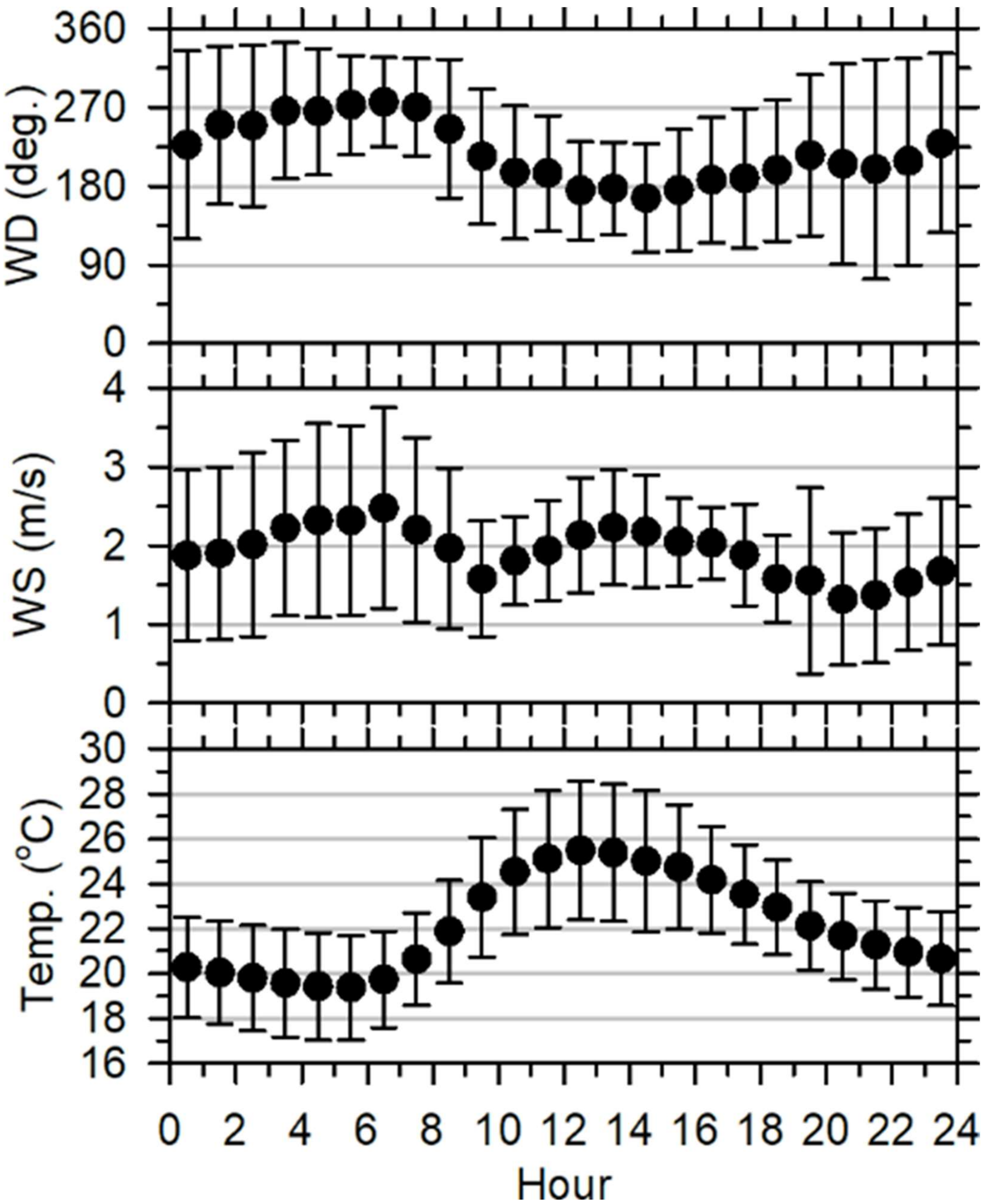

SFig. 1 Mean diurnal cycles of wind direction (WD), wind speed (WS), and air temperature during the observation period. Error bars show standard deviations.

Supplement 2

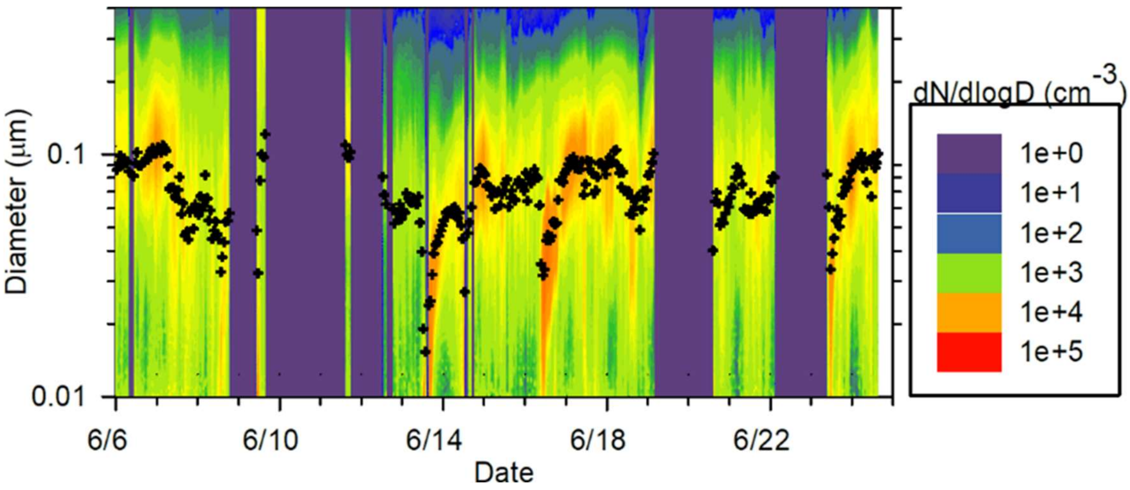

SFig. 2 Time series of size distributions (shading) and mode diameters (dots) of aerosol particles during the observation period.

Supplement 3

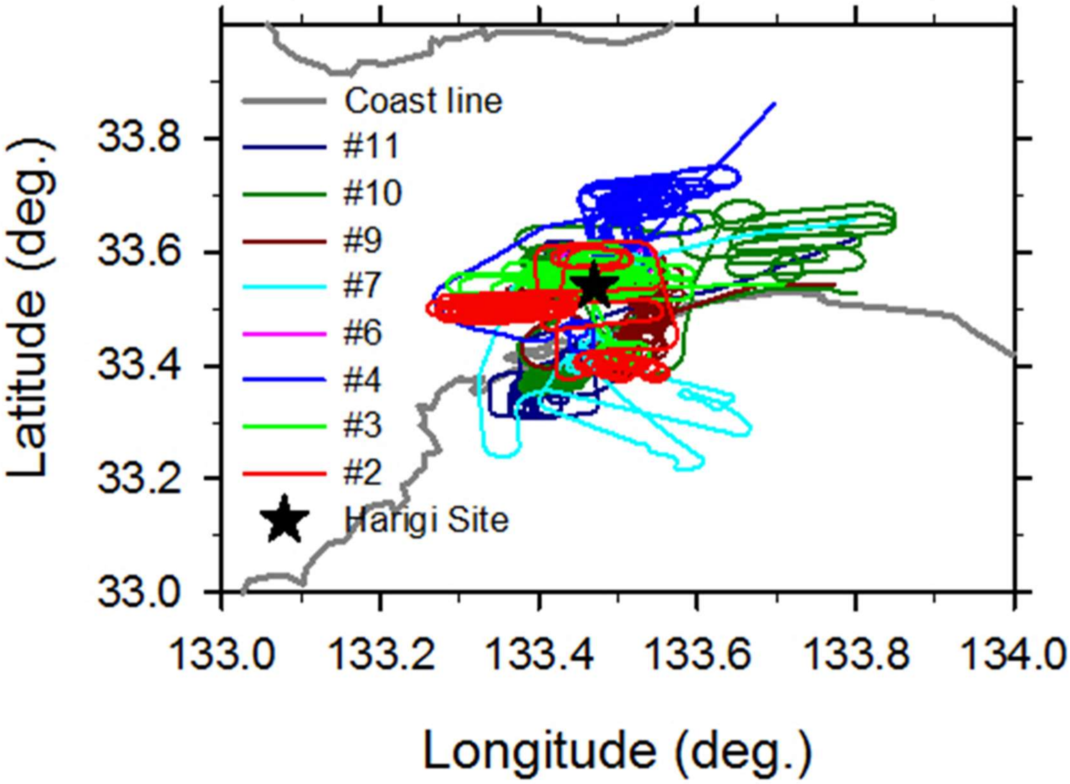

SFig. 3 Aircraft flight tracks that collected data used for comparison with ground-based measurements.